Geometry and Hydration Structure of Pt(II) Square Planar Complexes $[Pt(H_2O)_4]^{2+}$ and $[PtCl_4]^{2-}$ as Studied by X-ray Absorption Spectroscopies and Quantum-Mechanical Computations

Regla Ayala,[†] Enrique Sánchez Marcos,[†] Sofía Díaz-Moreno,[‡] V. Armando Solé,[‡] and Adela Muñoz-Páez*[,§]

Departamento de Química Física, Universidad de Sevilla, 41012-Sevilla, Spain, European Synchrotron Radiation Facility, 6 rue Jules Horowitz-BP 220, 38043 Grenoble Cedex 9, France, and Instituto de Ciencia de Materiales, Departamento de Química Inorgánica, CSIC−Universidad de Sevilla, c/ Americo Vespucio, 41092-Sevilla, Spain

Received: January 25, 2001; In Final Form: April 26, 2001

The geometrical structure of the tetraaquo and tetrachloro Pt(II) complexes in aqueous solutions has been studied by means of X-ray absorption spectroscopies (EXAFS and XANES), combined with quantum-mechanical computations. The latter were carried out to supply independent information about the arrangement of water molecules around the complexes. To this aim the $[PtCl_4]^{2-}\bullet(H_2O)_2$ and $[Pt(H_2O)_4]^{2+}\bullet(H_2O)_8$ structures were optimized and the XANES spectra computed using this theoretical structural information were compared with the experimental spectra. From this comparison it was deduced that the hydration shell of the tetraaquo complex was responsible for a small feature of the XANES spectrum above the white line. Pt−Cl distance in $[PtCl_4]^{2-}$ units, both in the crystalline compound, K_2PtCl_4, and in aqueous solution, was found to be 2.30 Å. Pt−O distance in $[Pt(H_2O)_4]^{2+}$ species was 2.02 Å. No evidence of stable axial water molecules was found in the aquo complex case. Quantum-mechanical optimization of $[PtCl_4]^{2-}\bullet(H_2O)_2$ aggregate indicated that water molecules adopt axial orientation with a Pt−O distance of 3.3 Å.

Introduction

Most stable cations of transition metals form well-defined hydrates whose structure has been solved both in solution and the solid state.[1] The most frequent hydration number is six, but higher coordination numbers, such as nine (La(III)), eight (Y(III)),[2] or seven (Sc(III)),[3] although it is still controversial,[4] can also be found. Conversely, lower coordination numbers are found for group-10 divalent cations, Pt(II) and Pd(II), where the highly favored square planar geometry points to the existence of four-coordinated hydrates for both cations. Elding et al. have carried out, thorough studies devoted to the synthesis and isolation,[5] spectroscopic characterization[6] and elucidation of the mechanism of ligand substitution processes of both aqua ions. These results are compatible with square planar geometry. Nevertheless, synthesis and characterization of solid-state crystalline hydrate has not been reported so far. Likewise, structural determinations in aqueous solutions are scarce. This might be due to the low yield in their synthesis, particularly in the case of Pt(II) hydrate, what is probably related to the stability of the complex, lower than that of tetrachloride or tetraammine Pt(II) complexes.[7] This has prevented the use of large angle X-ray Scattering (LAXS) spectroscopy in solution. Using extended X-ray absorption fine structure (EXAFS) spectroscopy, a technique which has shown to be useful in the structural investigation of dissolved species,[8] aqueous solutions containing $[Pt(H_2O)_4]^{2+}$ species have been measured, obtaining a value of 2.01 Å for Pt−O coordination distance.[9] More attention has been devoted to other Pt(II) square planar complexes, tetrachloride or tetraammine, due to their applications as precursors of heterogeneous catalyst, or as intermediates in the synthesis of anticancerigen species, such as the *cis*-diamminedichloro Pt-(II) complex.[10]

In addition to the determination of the structure of the square planar complex, an interesting issue concerning these complexes is the elucidation of the presence of axially coordinated weakly bonded solvent molecules. These axial molecules, in case they exist, could play a major role in the reactivity of these complexes, for which ligand substitution reactions usually take place via an associative mechanism.[11,12] Hellquist et al. did not find any evidence of the existence of such axial solvent molecules in dimethyl sulfoxide solutions by using the LAXS technique.[9] In contrast to this finding, Caminiti et al., on the basis of results from the same technique, propose the existence of axially bound water molecules in aqueous solutions containing $[PtCl_4]^{2-}$ species, the distance Pt−O being equal to 2.77 Å.[13]

The near edge region of the X-ray absorption spectra (XANES) contains information about coordination geometries and medium range order in condensed media.[8] Consequently, it has been used in the investigation of the aquo complexes,[14] helping sometimes in the conflicting determination of the hydration number[2] or the localization of light atoms such as hydrogen.[15,16] Nevertheless, in all these studies, most of them devoted to octahedral hydrates, only the first hydration shell has been taken into account, considering either $[MO_6]^{10-}$ or $[MO_6H_{12}]$ clusters. The effect of additional water molecules from the solvent has been neglected, probably because detailed

* Corresponding author. Fax: 34-95-4460665. E-mail: adela@cica.es.
[†] Departamento de Química Física. Universidad de Sevilla.
[‡] European Synchrotron Radiation Facility.
[§] Instituto de Ciencia de Materiales, Departamento de Química Inorgánica, CSIC−Universidad de Sevilla.

10.1021/jp010326+ CCC: $20.00
Published on Web 07/13/2001

structural information is required to carry out these computations, an information of involved access. This problem can be overcome by using as a source of structural information the optimized geometries from quantum mechanical computations.

Herewith we present a structural study of the Pt(II) square planar complexes, tetraaquo, $[Pt(H_2O)_4]^{2+}$, and tetrachloro, $[PtCl_4]^{2-}$, both in aqueous solution, combining the quantum-mechanical computations and X-ray absorption spectroscopies, EXAFS and XANES. To test the suitability of the methodology used in the analysis (e.g., phase shift and backscattering amplitude functions in the EXAFS analysis), the related solid compound of known structure, $K_2[PtCl_4]$, has been analyzed in the same way, and its structure used as an alternative geometry for the XANES computations. The highly symmetric environment around Pt(II) cations in both complexes might emphasize multiple scattering (MS) contributions to the EXAFS spectra, as already observed in other hydrates[14,17] and halo complexes.[18] For this reason, these contributions have been analyzed as well, using the appropriate models[19] to keep to a minimum the number of fitting parameters. The structural information obtained from the quantum mechanical computations was compared with that obtained from the EXAFS analysis.

Methods

Sample Preparation. $[Pt(H_2O)_4]^{2+}$ was synthesized by acid-catalyzed aquation of $[PtCl_4]^{2-}$, which yields mainly $[PtCl(H_2O)_3]^{+}$, followed by slow addition of a solution containing Ag(I) cations to remove the remaining chloride anions.[1c,5] Solutions containing this complex can be standardized using the absorbance at 273 nm ($\epsilon = 56.6\ M^{-1}\ cm^{-1}$). Solutions approximately 5×10^{-3} M in $[Pt(H_2O)_4]^{2+}$ species were obtained. $K_2[PtCl_4]$, from Aldrich Chem., was used to record the spectrum of the solid compound. Aqueous solutions were prepared by dissolving it in 0.1 M $HClO_4$ to obtain the spectrum of $[PtCl_4]^{2-}$(aq) species (salt concentration was 0.1 M).

X-ray Absorption Measurements. Pt L_{III} edge XAS spectra were measured at the Synchrotron Radiation Source, E.S.R.F., beamline ID26[20] using the U42m undulator, in fluorescence mode, using a Si photodiode operating in current mode as detector with a six absorption-length filter supplied by EXAFS Materials. The ring was operating at 6 GeV in 16 bunches mode ($I = 60-90$ mA). A Si(220) double crystal monochromator was used. A Pt foil was used as an internal energy calibration. To improve the signal-to-noise ratio several quick EXAFS scans (lasting 39 s), between 45 and 90, were recorded. Measurements were carried out in a Teflon liquid cell, 1 mm path length, with polyacetylene windows, at around 3 °C to avoid evaporation of the solvent. pH was kept below 1 to prevent hydrolysis and polymerization.

XANES Computation and EXAFS Data Analysis. Full multiple-scattering (FMS) calculations were carried out to compute the XANES region of the XAS spectra, using the self-consistent muffin tin potential and the real-space multiple-scattering procedure as implemented in the FEFF program (version 8.10).[21] The self-consistent field procedure (SCF) employed allows the determination of individual potentials for each type of atom on the basis of purely ab initio calculations of the electronic structure of the cluster considered. The Hedin-Lundqvist exchange and correlation potential was used, a potential previously used in similar systems.[15,22] It has been reported that the consideration of hydrogen atoms in the computation of the XAS spectra with the FEFF code led to unsatisfactory reproduction of them.[23,24] Difficulties are mainly associated with an overestimation of the backscattering contribution, but this does not affect their role in the self-consistent field calculation of the potential.[25] Therefore, hydrogen atoms were considered to compute the potential of the different types of atoms of the hydrated structures. In this way, Fermi level and polarization effects on the absorber and backscatterer atoms are computed under the influence of hydrogen atoms. Other authors have observed as well the effect of hydrogen in the XANES spectra through the modification of the electronic state of the host atoms.[15,16]

To extract the EXAFS function from the X-ray absorption spectrum, edge energy was determined as the maximum of the first derivative of the X-ray absorption spectra. Background subtraction was carried out taking into account the Cook and Sayers criteria[26] by the procedure described elsewhere[27] using the XANADU analysis package. Normalization was done dividing by the edge step. The phase shift and backscattering amplitude functions used in the EXAFS analysis were calculated with the FEFF program.[21] EXAFS data were analyzed with the FEFFIT 2.35 software package.[28]

Quantum-Mechanical Computations. Structures of chloro and aquo Pt(II) complexes were optimized at the MP2 level using the Dolg et al. relativistic effective core potential for the Pt atom.[29] The *sdd* basis sets were used for the Pt atom, and *cc-pvdz*[30] for the other atoms of the cluster. In the case of chlorocomplexes basis sets were augmented by diffuse functions (*aug-cc-pvdz*), to improve the description of negatively charged complexes.[31] Calculations were carried out by means of the Gaussian-98 program.[32]

TABLE 1: Optimized Geometrical Parameters Obtained from Quantum-Mechanical Computations at the MP2 Level for $[Pt(H_2O)_4]^{2+}$ and $[PtCl_4]^{2-}$ Complexes and Their Hydrated Forms

geometrical parameter[a]	$[PtCl_4]^{2-}$	$[PtCl_4]^{2-}$-$(H_2O)_2$	$[Pt(H_2O)_4]^{2+}$	$[Pt(H_2O)_4]^{2+}$-$(H_2O)_8$[b]
$R(Pt-X_I)$ (Å)	2.364	2.352	2.049	2.032 (2.020)
$R(Pt-H_I)$ (Å)			2.729	2.647 (2.684)
$R(Pt-O_{II})$ (Å)		3.288		3.935 (3.977)
$R(Pt-H_{II})$ (Å)		2.751		4.536 (4.621)
$R(O_I-H_I)$ (Å)		0.974	0.974	0.996 (0.994)

[a] Subscripts "I" and "II" refer to atoms belonging the first and second coordination shell, respectively. [b] Values correspond to the C_2-symmetry and D_4-symmetry (in parenthesis) structures.

Results

Quantum-Mechanical Geometries of the Complexes. Table 1 collects the main geometrical parameters of the optimized geometry for the tetraaquo and tetrachloride Pt(II) complexes both isolated (column 2 and 4) and with a solvation shell (columns 3 and 5). For the isolated complexes, the obtained Pt−Cl distance was 2.36 Å, 0.06 Å larger than the reported value for the crystalline compounds,[33] whereas the Pt−O distance was 2.05 Å, 0.04 Å larger than the value obtained by Hellquist et al. from the EXAFS measurements.[9] The lengthening in coordination distances of the isolated complexes might be, at least in part, a consequence of the condensed medium effects, which usually cause a shortening of the metal−ligand distances. Regarding theoretical computations, Deeth and Elding, using DFT calculations, obtain for the tetraaquo complex a distance of 2.04 Å,[34] and Burda et al. by means of the G3 method find a Pt−Cl distance of 2.33 Å for the $[PtCl_4]^{2-}$ complex.[35]

In addition to the determination of the isolated structures, a detailed investigation of the preferred site for water molecules

interaction around the planar complexes was carried out. This was done to check the influence on the XANES spectra of the medium range order solvation structure. The obtained geometries for the aggregates including water molecules has been collected in Table 1 as well.

Due to the different net charge of the complexes studied and to the small backscattering effect of atoms beyond the first solvation sphere on the XAS spectra, two different types of hydrated structures have been examined for the tetrachloride and tetraaquo complexes. In the case of the tetrachloride, only axial arrangements of water molecules were investigated. In equatorial solvation of chloride ligands, oxygen atoms are too far away to give relevant contributions to the XANES spectrum. Thus, the geometry of $[PtCl_4]^{2-}\cdot(H_2O)_2$ supermolecule was optimized, finding a structure where the two axial water molecules orientate their hydrogen atoms pointing symmetrically to two chloride anions of the square planar complex. Each water molecule eclipses two opposite Pt−Cl bonds, and water molecule planes are mutually staggered (Figure 1A). In agreement with the condensed medium effects described above, due to the specific $[PtCl_4]^{2-}-H_2O$ interaction, Pt−Cl distance shortens 0.012 Å with respect to the value in the isolated complex. The minimum in the potential energy surface for water molecules in the axial region appears for a Pt−O distance of 3.3 Å. This distance is much larger than that obtained by Caminiti, 2.77 Å,[13] so that oxygen atoms, which could yield an additional backscattering contribution to the EXAFS spectrum, are 1 Å further from the absorbing Pt atoms than the chloride ligands.

For the $[Pt(H_2O)_4]^{2+}$ complex, it was not possible to find stabilizing regions for water molecules at axial positions. In fact, a significant number of starting points with different arrangements always led to the migration of water molecules toward the second hydration shell in the equatorial region, forming hydrogen bonds with the first-shell water molecules of the planar complex. For the sake of completeness, two structures of the Pt(II) tetrahydrate complex solvated by an additional hydration shell, i.e., $[Pt(H_2O)_4]^{2+}\cdot(H_2O)_8$, were investigated. A first minimum was located for a D_4-symmetry when second shell water molecules were constrained among them to adopt the same orientation with respect to their corresponding first-shell water molecule (Figure 1B). A second minimum was found when this restriction was released, what led to a C_2-symmetry structure (Figure 1C), which is 6 kcal/mol more stable than the previous one. The main geometrical parameters of these two structures have been collected in Table 1. As observed in the case of the tetrachloride complex, the interaction of the water molecules from the second hydration shell with the water molecules of the $[Pt(H_2O)_4]^{2+}$ units, through hydrogen bonds, shortens the $Pt-O_I$ distance by 0.02−0.03 Å. For this second hydration shell the $Pt-O_{II}$ distance is 3.95 Å, on average. The investigation of the axial region for this complex indicated that no potential well is present; even when the equatorial second shell was already completed, axial water molecules were not stable. Therefore, the persistence of axial water arrangement is not expected, and consequently no spectroscopic features, either in the XANES or EXAFS regions, derived from it.

XANES. Figure 2 includes the XANES region of the experimental X-ray absorption spectra of $K_2[PtCl_4]$ in the solid state (solid line) and the calculated ones for clusters of different sizes (dotted lines). The XANES spectra were computed using the FEFF program and the geometry has been taken from the crystal structure obtained from XRD data.[33] Selected cluster sizes correspond to the Pt absorbing atom surrounded by an increasing number of coordination shells. An intermediate computation for a 33-atom cluster yielded a spectrum very similar to the one computed for the 133-atom cluster. Similarly, Ankudinov et al. reported XANES computations up to a 39-atom cluster, indicating that changes were negligible for larger cluster sizes.[36]

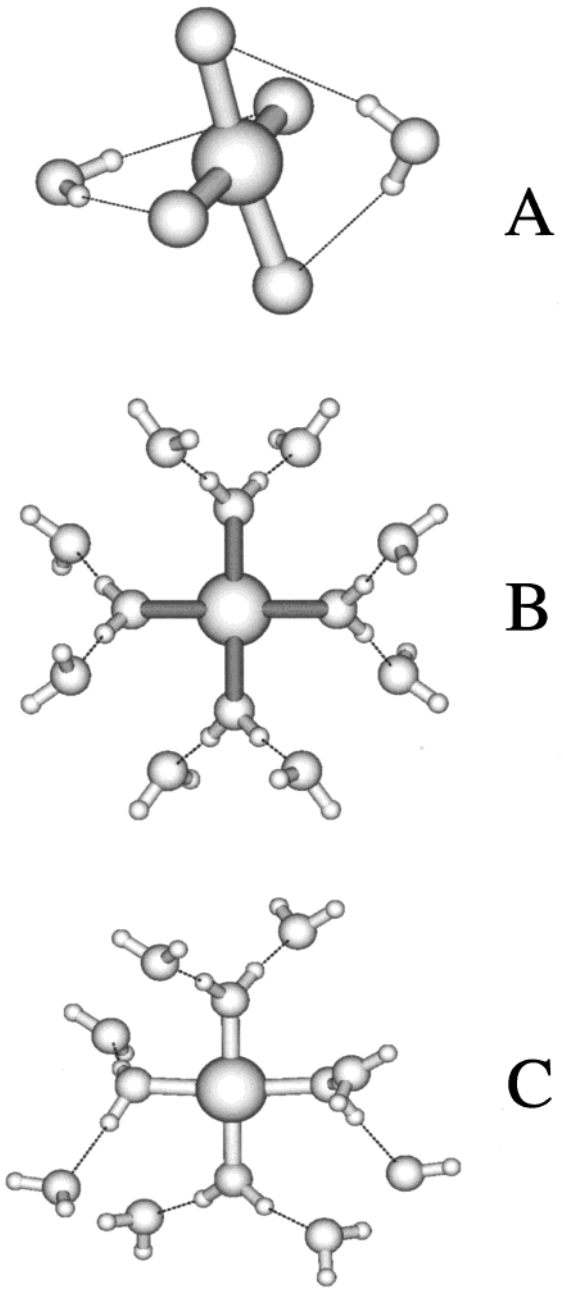

Figure 1. MP2 optimized geometries for **(A)** $[PtCl_4]^{2-}(H_2O)_2$, **(B)** $[Pt(H_2O)_4]^{2+}(H_2O)_8$ with D_4 symmetry, and **(C)** $[Pt(H_2O)_4]^{2+}$ $(H_2O)_8$ with C_2 symmetry.

An examination of the trend of the computed XANES with the cluster size shows that the features of the spectrum are more defined when the cluster size increases. The spectrum computed for the 133-atom cluster resembles more the experimental spectrum. Note the small peak at 11583 eV, the shoulder at 11595, and the broad peaks at around 11635 and 11680 eV. The main difference between the computed and experimental spectra is the small feature appearing at 11577 eV in the experimental spectrum which is not well resolved in the computed one, although a change in the slope of the white line

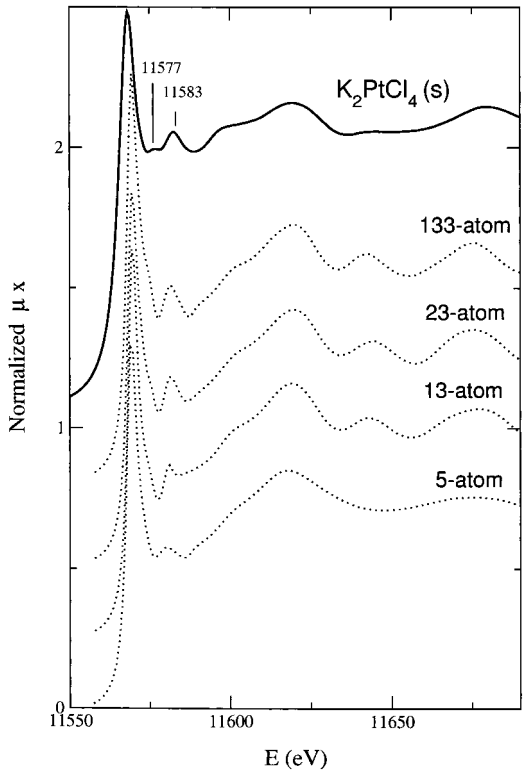

Figure 2. XANES region of the Pt-L_{III}-edge X-ray absorption spectra of $K_2[PtCl_4]$. Solid line: experimental spectra of the complex registered in solid state. Dotted lines: spectra calculated for cluster formed by 5, 13, 23, and 133 atoms using the geometry of the crystalline compound.[33] Energy axis has been shifted +5 eV for the computed spectra.

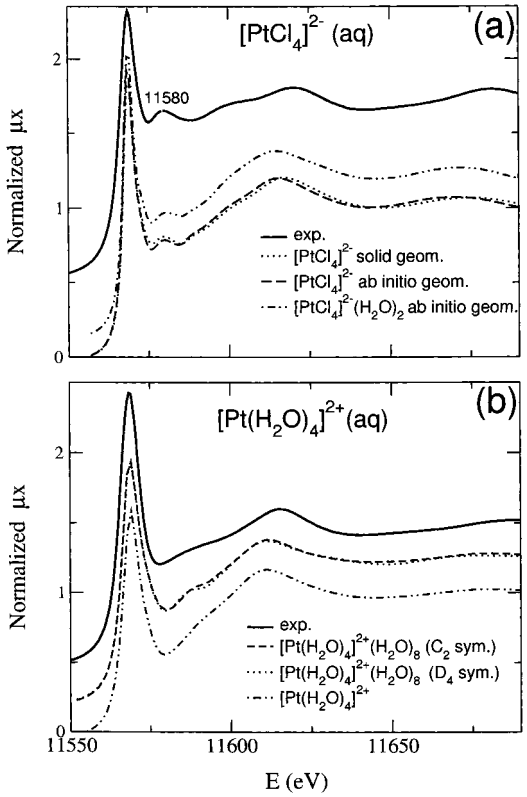

Figure 3. XANES region of the Pt-L_{III}-edge X-ray absorption spectra of complexes in aqueous solution, **(a)** $[PtCl_4]^{2-}$(aq) and **(b)** $[Pt(H_2O)_4]^{2+}$-(aq). Solid lines: experimental data. Nonsolid lines: computed spectra using the indicated geometries. Energy axis has been shifted +5 eV for the computed spectra.

could be due to the convolution of this small feature. The tendency observed in the cluster sequence confirms the general assumptions made in the computations of the XANES spectra, according to which medium- and long-range order should be taken into account, so that increasing the cluster sizes of the appropriate structures should improve the accuracy of the reproduction of the spectrum, when solid state is considered.

Figure 3 shows the experimental (solid lines) and computed XANES spectra for the chloro and aquo complexes in aqueous solution with and without hydration shell. The experimental spectra of $[PtCl_4]^{2-}$ in aqueous solution (Figure 3a) is rather similar to the corresponding experimental spectrum of the solid $K_2[PtCl_4]$ (Figure 2). The main difference appearing above the white line. For the solution species a small peak appears at 11580 eV, a feature which splits for the solid system into two peaks, a smaller one at 11577 eV and a bigger one at 11583 eV. The computed XANES spectra of the $[PtCl_4]^{2-}$ complex using both the optimized MP2 geometry (Pt−Cl distance = 2.35 Å) and that of the crystal structure (Pt−Cl distance = 2.308 Å) have also been plotted in Figure 3a.[33] The shortening of 0.04 Å in Pt−Cl distance slightly modifies the spectrum, shifting the main peak above the white line to higher energies, as already observed by Bianconi et al. in computations of XANES spectrum of iron hexacyanide complexes.[37] Finally, the computed spectrum obtained from the ab initio structure of $[PtCl_4]^{2-}\cdot(H_2O)_2$ shows that the influence on the spectrum of the two axial water molecules is negligible.

Figure 3b includes the experimental XANES spectrum for the Pt(II) tetrahydrate in aqueous solution and those computed using the optimized geometry for the $[Pt(H_2O)_4]^{2+}$ complex and the two structures with hydration shell (C_2 and D_4 symmetry), $[Pt(H_2O)_4]^{2+}\cdot(H_2O)_8$, described in Table 1 and plotted in Figure 1. It is worth noting how the inclusion of the hydration shell causes a change in the shape of the spectrum, generating a shoulder at ca. 11587 eV, between the white line and the main resonance peak at 11610 eV. This is also observed in the experimental spectrum, although the statistical contribution of many structures damp its form with respect to the computed one, that is derived from a single structure. A final remark concerns the almost negligible effect on the XANES spectrum of the change in the structure of the hydrated complex considered (dashed vs dotted line in Figure 3b).

The feature appearing at 11583 and 11580 eV in the spectra of the tetrachloride complexes, both experimental and calculated, is very similar to the one found by Ankudinov et al. in the XANES spectra of Pt(II) and Pt(IV) chlorides, and ascribed by these authors to a hybridization peak resulting from the combination of the photoelectron state and occupied atomic Cl 3d-states.[36] The electronic nature of this feature is supported by the fact that the feature does not appear in the corresponding spectra of the aquo complexes.

EXAFS. The raw data of $[Pt(H_2O)_4]^{2+}$ and $[PtCl_4]^{2-}$ complexes in aqueous solutions, and the K_2PtCl_4 compound in solid state appear in Figure 4a and 4b. Noise level is much higher in the first case than in the halide complexes. The two spectra of the Pt(II) halide are very similar, showing only small differences at around 4.5 and 6.0 $Å^{-1}$ (Figure 4b). The magnitude of the corresponding Fourier transforms, included in Figure 4c, shows a first peak appearing at 2.0 and 2.3 Å, attributable to Pt−O and Pt−Cl contributions, respectively. In the halide complexes a second small peak appears between 4 and 5 Å. In the solution species it could be due either to a second hydration shell or to a MS contributions within the first coordination shell. In the

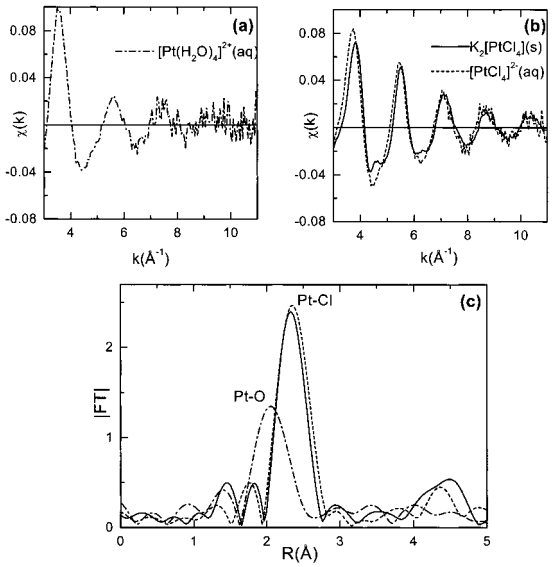

Figure 4. Pt-L_{III}-edge experimental EXAFS spectra of **(a)** $[Pt(H_2O)_4]^{2+}$(aq) (dashed−dotted line); **(b)**$[PtCl_4]^{2-}$(aq) (dashed line) and solid $K_2[PtCl_4]$, (solid line). **(c)** Magnitude of the Fourier transform of the EXAFS spectra included in Figure 4a, Pt−O phase corrected, dashed−dotted line and in Figure 4b, Pt−Cl phase corrected, dashed and solid lines for dissolved and solid species, respectively.

TABLE 2: Best Fit Parameters Obtained from the Analysis of the Pt-L_{III}-edge EXAFS spectra of the $[Pt(H_2O)_4]^{2+}$, $K_2[PtCl_4]$ in Solid State and in Aqueous Solution[a]

	$[Pt(H_2O)_4]^{2+}$(aq)	$[PtCl_4]^{2-}$ (aq)	$K_2[PtCl_4]$ (s)
R(Pt−X) (Å)	2.02 ± 0.015	2.304 ± 0.005	2.300 ± 0.005
$\sigma_1 2$ (Pt−X) (Å^2)	0.003 ± 0.001	0.0021 ± 0.0004	0.0028 ± 0.0004
R(Pt−K) (Å)			4.09 ± 0.05
$\sigma_1 2$ (Pt−K) (Å^2)			0.02 ± 0.01
ΔE_o (eV)	6 ± 2	9.6 ± 0.8	8.5 ± 0.6
r	0.08	0.024	0.05
χ^2_{red}	4.8	1.4	10.6
Δk	2.8−10.4	2.8−11.5	2.8−11.5
ΔR	1.1−3.9	1.1−4.9	1.1−5.4
noise amplitude	0.007	0.003	0.001

[a] ΔE_0: Inner potential correction; σ_n^2: Debye−Waller factors; R: coordination distances; **r** and χ^2_{red}: goodness of fit parameters (see ref 28).

solid compound, K_2PtCl_4, several SS contributions might appear between 4 and 5 Å, e.g., those corresponding to the coordination shells formed by eight K atoms at 4.08 Å, two Pt atoms at 4.14 Å, and/or eight Cl atoms at 4.74 Å. All these shells could contribute to the second peak in the FT of the solid as well as the MS phenomena within the first coordination shell.

A reasonable reproduction of the spectrum of the aquo complex could be achieved with a Pt−O single scattering contribution with parameters included in Table 2, corresponding to a symmetric square planar complex with four water molecules at 2.02 ± 0.015 Å. This value is, within the limits of accuracy, the same than that obtained from the quantum-mechanical calculations (2.03 Å) and that the value previously reported by Hellquist et al. (2.01 Å).[9] Since the complex is kinetically stable (unimolecular rate constant for water release from the first hydration shell $k = 4 \times 10^{-4}$ s^{-1}),[11] the second hydration sphere water molecules were expected to be stable enough to be detected. Nevertheless, data quality prevented the accurate analysis of EXAFS contributions beyond the main shell with new fitting parameters. Fit quality in k space improves by taking into account the most intense MS contributions, those corresponding to paths 2, 3, and 4 in Scheme 1, for which Debye−

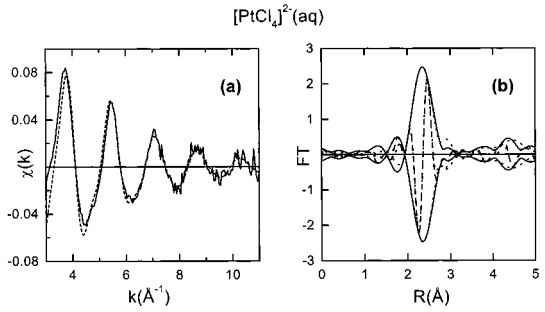

Figure 5. (a) Pt-L_{III}-edge experimental EXAFS spectra of $[PtCl_4]^{2-}$(aq) (solid line) and best fit with the parameters included in Table 2 (dashed line). **(b)** Magnitude and imaginary part of the Pt−Cl phase corrected Fourier transform of the spectra included in Figure 4a.

SCHEME 1: Scattering Paths Used in the EXAFS Analysis

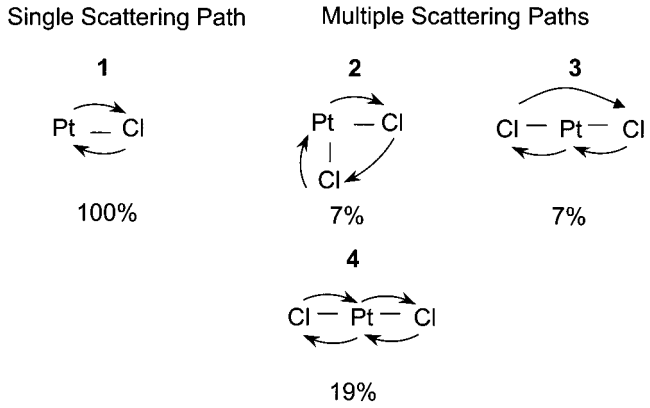

Waller (DW) factors are twice the value of the DW factor of the first shell SS path. This value is similar to that obtained in the hexahydrates of divalent and trivalent transition metal cations.[17b]

The best fit (see parameters in Table 2 and Figure 5) obtained for the spectra of the dissolved ($[PtCl_4]^{2-}$)(aq) species is achieved by considering the contributions arising from the first coordination shell formed by four chlorine atoms located at 2.304 Å, a value very close to that obtained in XRD studies of the crystalline compounds, 2.308 Å, and slightly smaller than that reported by Caminiti et al. in an X-ray scattering study of an aqueous solution containing $[PtCl_4]^{2-}$ species, 2.315 Å. The same MS contributions considered in the aquocomplex must be taken into account to attain a good fit, e.g., those arising from paths 2, 3, and 4, although in this complex, triangular path number 3 showed an unexpected high intensity requiring the same DW factor than that of the SS path number 1. In contrast with that observed by Caminiti et al.,[13] no contribution from axial water molecules located at around 2.8 Å appeared in the EXAFS spectrum, what agrees with the quantum-mechanical computations of the hydrated complex and with the XANES spectrum.

The spectrum of the solid compound was fitted adding only one SS contribution, arising from a coordination shell formed by eight K atoms at 4.09 Å, to the MS ones considered to fit the spectrum of the $[PtCl_4]^{2-}$(aq) species. The best fit parameters, included as well in Table 2, are very close to those of the complex in solution, except that the Pt−Cl distance is slightly shorter and the SS DW factor is slightly higher for the solid system. Although the expected change is just the opposite, we observed a similar change in the DW factor of the solid system in a recent XAS study of the $K_2[Ni(CN)_4]$ species.[22]

Concluding Remarks

The Pt(II) aquo complex has a square planar geometry, oxygen atoms being located at 2.02 Å. Similarly, $[PtCl_4]^{2-}$ units, both in aqueous solution and the solid state, are square planar, Pt−Cl distance being 2.30 Å. The MS contribution arising from triangular path (path 2 in Scheme 1) has an intensity higher than that found in octahedral complexes since its Debye−Waller factor is the same than that of the main SS path.

The solvation shell of the Pt(II) aquo complex is formed by eight water molecules hydrogen bonded to the water molecules within the tetraaquo complex in an equatorial arrangement ($Pt-O_{II} \sim 3.95$ Å).

From the analysis of the EXAFS data, and from the combined quantum-mechanical and XANES spectra computations, it can be deduced that the axial region of these square planar complexes in solution does not present a potential well which favors restricted orientation of water molecules, so that no coherent contribution to the X-ray absorption spectra is detected either in the EXAFS or in the XANES spectra of the $[PtX_4]^{2+/-}$ ($X = Cl^-$, H_2O) complexes.

Previous ascription[36] of a hybridization peak in the Pt−Cl XANES spectrum, involving d-atomic Cl orbitals, is supported by this study, where such a peak is observed for experimental and computed spectra of chloro complexes in solid state and aqueous solution, but it does not appear in the corresponding spectra of the aquo complex, in which there are only Pt−O contributions.

Acknowledgment. We thank Prof. J. J. Rehr, University of Washington, for supplying us with a released version of the FEFF program. ESRF is acknowledged for beam allocation at the beamline ID26 and Fundación Ramón Areces, XI Programa Nacional of Spain for financial support.

References and Notes

(1) (a) Ohtaki, H.; Radnai, T. *Chem. Rev.* **1993**, *93*, 115. (b) Marcus, Y. *Chem. Rev.* **1988**, *88*, 1475. (c) Richens, D. T. *The Chemistry of Aqua Ions*; John Wiley & Sons: New York, 1997.

(2) Diaz-Moreno, S.; Chaboy, J.; Muñoz-Paez, A. *J. Phys. Chem. A* **2000,** *104*, 1278.

(3) Yamaguchi, T.; Niihara, M.; Takamuku, T.; Wakita, H.; Kanno, H. *Chem. Phys. Lett.* **1997**, *274*, 485.

(4) Rudolph, W. W.; Pye, C. C. *J. Phys. Chem. A* **2000**, *104*, 1627.

(5) (a) Elding, L. I. *Inorg. Chim. Acta* **1976**, *20*, 65. (b) Elding, L. I. *Acta Chim. Scand.* **1970**, *24*, 1331.

(6) Elding, L. V.; Olsson, L. F. *J. Phys. Chem.* **1978**, *82*, 69.

(7) *Comprehensive Coordination Chemistry*; Pergamon Press: Oxford, 1987; Vol. 4, Chapter 13.7, p 261.

(8) Stern, E. A. In *X-ray Absorption: Principles, Applications, Techniques of EXAFS, SEXAFS and XANES*; Koningsberger, D. C., Prins, R., Eds.; Wiley-Interscience: New York, 1988; p 3.

(9) Hellquist, B.; Bengtsson, L. A.; Holmberg, B.; Hedman, B.; Persson, I.; Elding, L. I. *Acta Chem. Scand.* **1991**, *45*, 449.

(10) (a)Muñoz-Paez, A.; Koningsberger, D. C. *J. Phys. Chem.* **1995**, *99*, 4193. (b) Rosenberg, B.; van Camp, L.; Trosko, J. L.; Mansour, V. H. *Nature (London)* **1969**, *222*, 385. (c) Reedijk, J. *Chem. Commun.* **1996**, *7*, 801.

(11) Helm, L.; Elding, L. I.; Merbach, A. E. *Inorg. Chem.* **1985**, *24*, 1719.

(12) Deeth, R. J.; Elding, L. I. *Inorg. Chem.* **1996**, *35*, 5019.

(13) Caminiti, R.; Carbone, M.; Sadun, C. *J. Mol. Liq.* **1998**, *75*, 149.

(14) (a) Garcia, J.; Bianconi, A.; Benfatto, M.; Natoli, C. R. *J. Phys (France)* **1986**, *Colloq 47*, C9−49. (b) Benfatto, M.; Natoli, C. R.; Bianconi, A.; Garcia, J.; Marcelli, A.; Fanfoni, M.; Davoli, I. *Phys. Rev. B* **1986**, *34*, 5774.

(15) Benfatto, M.; Solera, J. A.; Chaboy, J.; Proietti, M. G.; Garcia, J. *Phys. Rev. B* **1997**, *56*, 2447.

(16) Chaboy, J.; Marcelli, A.; Bozukov, *J. Phys.: Condens. Matter* **1995**, *7*, 8197.

(17) (a) Filiponi, A.; D'Angelo, P.; Viorel Pavel, N.; Di Cicco, A. *Chem. Phys. Lett.* **1994**, *225*, 150. (b) Sakane, H.; Muñoz-Páez, A.; Díaz-Moreno, S.; Martínez, J. M.; Pappalardo, R. R.; Sánchez Marcos, E. *J. Am. Chem. Soc.* **1998**, *120*, 10397.

(18) Van der Gaauw, A.; Wilkin, O. W.; Young, N. A.; *J. Chem. Soc., Dalton Trans.* **1999**, 2405.

(19) (a)Yokoyama, T.; Kobayashi, K.; Ohta, T.; Ugawa, A. *Phys. Rev. B.* **1996**, *53*, 6111. (b) Haskel, D. Ph.D. Thesis, University of Washington, Seattle, WA, 1998. (c)Yokoyama, T.; Yonanoto, Y.; Ohta, T. *Phys. Rev. B.* **1996**, *54*, 6921.

(20) Signorato, R.; Solé, V. A.; Gauthier, C. *J. Synchrotron Radiat.* **1999**, *6*, 176.

(21) (a) Ankudinov, A.; Ravel, B.; Rehr, J. J.; Conradson, S. D. *Phys. Rev. B* **1998**, *58*, 7565. (b) Mustre de León, J.; Rehr, J. J.; Zabinsky, S. I.; Albers, R. C. *Phys. Rev. B* **1991**, *44*, 4146. (c) Zabinsky, S. I.; Rehr, J. J.; Ankudinov, A.; Albers, R. C.; Eller, M. J. *Phys. Rev. B* **1995**, *52*, 2995.

(22) Muñoz-Páez, A.; Díaz-Moreno, S.; Sánchez Marcos, E.; Rehr, J. J. Inorg. Chem. **2000**, *39*, 3784.

(23) Palmer, B. J.; Pfund, D. M.; Fulton, J. L. *J. Phys. Chem.* **1996**, *100*, 13393.

(24) Spångberg, D.; Hermansson, K.; Lindqvist-Reis, P.; Jalilehvand, F.; Sandström, M.; Persson, I. *J. Phys. Chem. B* **2000**, *104*, 10467.

(25) Campbell, L.; Rehr, J. J.; Schenter, G. K.; McCarthy, M. I.; Dixon, D. *J. Synchrotron Radiat.* **1999**, *6*, 310.

(26) Cook, J. W.; Sayers, D. E. *J. Appl. Phys.* **1981**, *52*, 5024.

(27) Sakane, H.; Miyanaga, T.; Watanabe, I.; Matsubayashi, N.; Ikeda, S.; Yokoyama, Y. *Jpn. J. Appl. Phys.* **1993**, *32*, 4641.

(28) Stern, E. A.; Newville, M.; Ravel, B.; Yacoby, Y.; Haskel, D. *Physica B* **1995**, *208&209*, 117.

(29) Andrade, D.; Haeussermann, M.; Dolg, M.; Stoll, H.; Preuss, H. *Theor. Chim. Acta* **1990,** *77*, 123.

(30) Dunnig, T. H., Jr. *J. Chem. Phys.* **1989**, *90*, 1007.

(31) Woon, D. E.; Dunnig, T. H., Jr. *J. Chem. Phys.* **1993**, *98*, 1358.

(32) Frisch, M. J.; Trucks, G. W.; Schlegel, H. B.; Scuseria, G. E.; Robb, M. A.; Cheeseman, J. R.; Zakrzewski, V. G.; Montgomery, J. A., Jr.; Stratmann, R. E.; Burant, J. C.; Dapprich, S.; Millam, J. M.; Daniels, A. D.; Kudin, K. N.; Strain, M. C.; Farkas, O.; Tomasi, J.; Barone, V.; Cossi, M.; Cammi, R.; Mennucci, B.; Pomelli, C.; Adamo, C.; Clifford, S.; Ochterski, J.; Petersson, G. A.; Ayala, P. Y.; Cui, Q.; Morokuma, K.; Malick, D. K.; Rabuck, A. D.; Raghavachari, K.; Foresman, J. B.; Cioslowski, J.; Ortiz, J. V.; Baboul, A. G.; Stefanov, B. B.; Liu, G.; Liashenko, A.; Piskorz, P.; Komaromi, I.; Gomperts, R.; Martin, R. L.; Fox, D. J.; Keith, T.; Al-Laham, M. A.; Peng, C. Y.; Nanayakkara, A.; Gonzalez, C.; Challacombe, M.; Gill, P. M. W.; Johnson, B.; Chen, W.; Wong, M. W.; Andres, J. L.; Gonzalez, C.; Head-Gordon, M.; Replogle, E. S.; Pople, J. A. *Gaussian 98, Revision A.7*; Gaussian, Inc.: Pittsburgh, PA, 1998.

(33) (a) Ohba, S.; Sato, S.; Saito, Y. *Acta Crystallogr. Sect. B* **1983**, *39*, 49. (b) Templetoon, D. H.; Templetoon, L. K. *Acta Crystallogr. Sect. A*, **1985**, *41*, 365.

(34) Deeth, R. J.; Elding L. I. *Inorg. Chem.* **1996**, *35*, 5019.

(35) Burda, J. V.; Zeizinger, M.; Sponer, J.; Leszczynski, J. *J. Chem. Phys.* **2000**, *113*, 2224.

(36) Ankudinov, A. I.; Rehr, J. J.; Bare, S. R. *Chem. Phys. Lett.* **2000**, *316*, 495.

(37) Bianconi, A.; Dell'Ariccia, M.; Durham, P. J.; Pendry, J. B. *Phys. Rev. B* **1982**, *26*, 6502.